The seismic stability and ductility of steel columns interacting with concrete footings

Hiroyuki Inamasu
Doctoral Assistant, Swiss Federal Institute of Technology (EPFL)
Lausanne, Switzerland
hiroyuki.inamasu@epfl.ch

Amit Kanvinde
Professor, University of California at Davis
Davis, United States of America
kanvinde@ucdavis.edu

Dimitrios Lignos
Associate Professor, Swiss Federal Institute of Technology (EPFL)
Lausanne, Switzerland
dimitrios.lignos@epfl.ch

ABSTRACT

First-story columns in steel moment resisting frames are subjected to various forms of geometric instabilities during earthquakes. These instabilities have the potential to seriously compromise structural performance, and expedite structural collapse. In turn, these instabilities are influenced by the interactions of the column boundary conditions. Of specific concern are base connections that involve embedding the column into a concrete footing. These connections are nominally assumed to be fixed, although recent experimental data suggests that they could be significantly flexible. A finite element parametric study examining the effect of connection flexibility on interior column seismic performance is presented. Several key variables, including column base flexibility, cross-section, axial load, and column length are interrogated. Results of the finite element study are presented in support of developing quantitative relationships between column base conditions and deformation capacity of the columns. Incorporation of these relationships into modeling frameworks is discussed.

1. Introduction

A number of recent experimental and numerical studies investigated the hysteretic response of wide flange steel columns in moment resisting frames (MRFs) under multi-axial cyclic loading

(Newell and Uang 2008; Suzuki and Lignos 2015; Uang et al. 2015; Elkady and Lignos 2015, 2016; Fogarty and El-Tawil 2016). In the studies by Elkady and Lignos (2016), the influence of the column end boundary conditions on the member hysteretic response was highlighted. Local and global geometric instabilities resulted into severe flexural strength deterioration and column axial shortening. In all cases the column was fixed at its base, which is a common assumption for columns embedded in a concrete footing.

Past experiments on embedded column base connections (Grilli et al. 2017) revealed that they have an appreciable flexibility due to the elastic deformation of the concrete subject to bearing stress, the base plate and the column embedment length. Notably, findings from reconnaissance reports from past earthquakes (Clifton et al. 2011; MacRae et al. 2015) as well as system-level numerical studies (Lignos et al. 2013) suggest that a flexible column base that may be partially damaged could enhance the seismic behavior of steel MRFs.

Although the influence of the column base flexibility on the structural behavior has only been investigated through nonlinear response history analyses (Zareian and Kanvinde 2013), its influence on the column member hysteretic response has never been examined.

This paper investigates the effect of the embedded column base connection flexibility on the column hysteretic behavior through rigorous nonlinear finite element (FE) simulations. A continuum FE model is first developed and validated with recent full-scale column tests. The steel columns utilize a variety of boundary conditions and cross-sectional characteristics. The FE model is then extended such that the column base flexibility can be considered. This flexibility is inferred on the basis of available full-scale tests on steel columns embedded on concrete footings. A parametric study is then conducted in which several key variables, including the column base flexibility, cross-section, axial load, and column length are interrogated. The influence of these variables on the column hysteretic behavior is highlighted through a number of illustrative examples.

2. Review of experimental data on wide flange steel columns and embedded columns in concrete footings

2-1. Recent experiments on wide-flange steel columns

Uang et al. (2015) tested twenty-five deep columns subjected to inelastic cyclic loading coupled with a constant compressive axial load and fixed end boundaries. They found that global and local slenderness ratios as well as the compressive axial load influence the observed failure modes that can vary from local to lateral torsional buckling.

Suzuki and Lignos (2015) examined the influence of the loading history on the seismic performance of cantilever wide-flange columns. Tests on nominally identical columns subjected to symmetric loading histories were complemented with monotonic and 'collapse consistent' loading histories that characterize the ratcheting behavior (Ibarra and Krawinkler 2005) a structure experiences prior to earthquake-induced collapse. They found that routinely used symmetric cyclic loading histories provide insufficient information regarding the deterioration characteristics of steel columns that primarily control structural collapse.

More recently, Elkady and Lignos (2016, 2017a) investigated the influence of boundary conditions on the seismic performance of interior wide flange steel columns with fixed-flexible boundary conditions. Referring to Figure 1a, columns with a flexible top boundary exhibit larger plastic deformation capacity compared to fixed end columns. The response of the latter is controlled by column axial shortening as shown in Figure 1b.
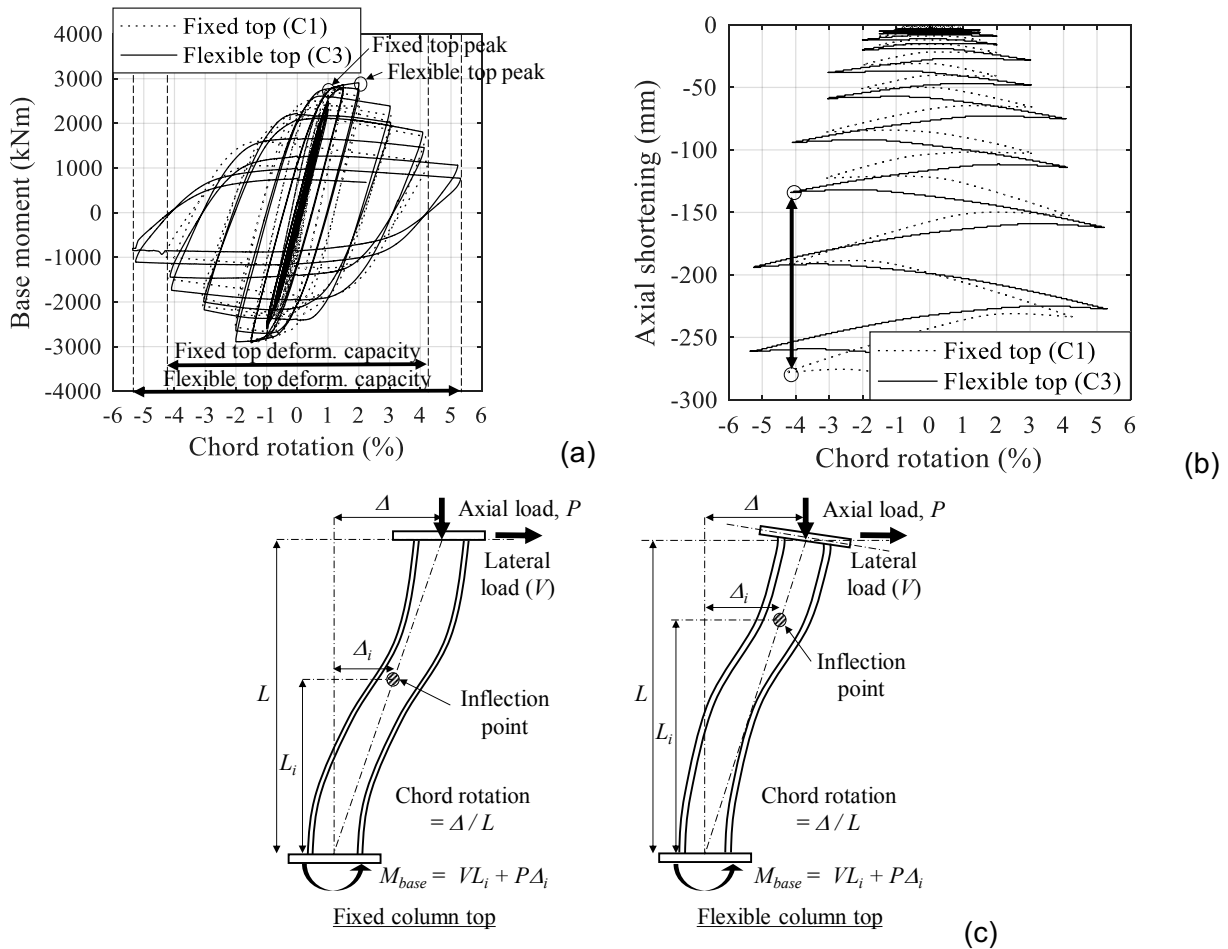
Figure 1 – Typical steel column hysteretic response and boundary conditions: (a) Moment-rotation relation; (b) axial shortening-rotation, and (c) deformed shapes (data from Elkady and Lignos 2016, 2017a).

2-2. Recent experiments on embedded column base connections

Grilli et al. (2017) recently investigated the seismic performance of embedded column base connections subjected to axial load, P, and lateral drift demands. Columns were designed to be elastic such that the observed failures were concentrated at the column base connection. Table 1 summarizes the main test parameters including the embedment depth, d_{embed}, and the applied axial load. The same table summarizes the measured maximum flexural strength, M_{max} and stiffness, β of the embedded column base connection (after subtracting the elastic contribution of the column). All the columns were tested in a cantilever fashion. Figure 2 illustrates the hysteretic response of a typical embedded column base connection. Table 1 as well as Figure 2 suggest that an embedded column base connection has an appreciable column base flexibility. The reported β values correspond to about 0.4 - 0.8% rotation under the design base moment.

It should also be noted that regardless of the column base flexibility, the specimens exhibited a considerable plastic deformation capacity without any strength loss.

Table 1 – Summary of embedded column base connection test data (Grilli et al. 2017)

Specimen ID	Column cross-section	Column length (m)	P (kN)	d_{embed} (mm)	M_{max} (kNm)	β (10^5kNm/rad)
#1	W14x370	2.84	445	508	2613	3.23
#2	W18x311	2.84	445	508	2324	3.84
#3	W14x370	3.10	0	762	3741	3.07
#4	W14x370	3.10	445	762	4124	3.38
#5	W14x370	3.10	-667*	762	3800	3.25

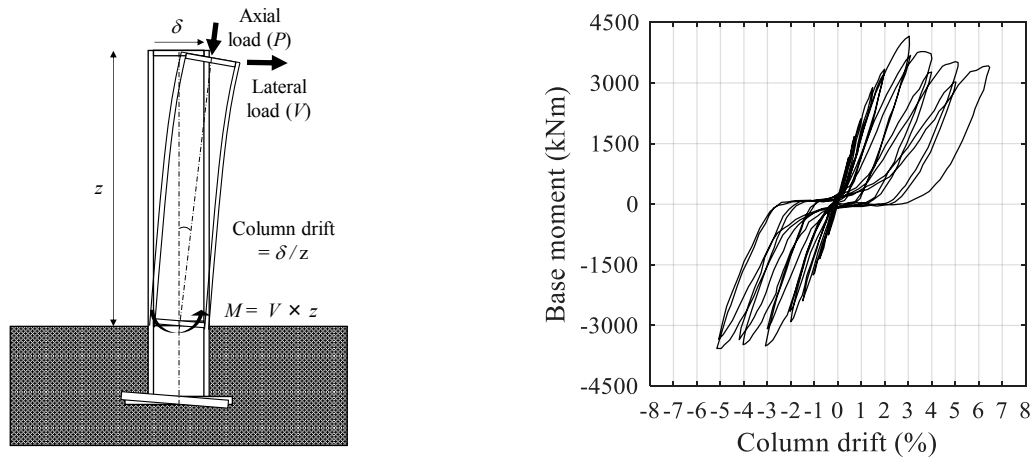* minus sign indicates tension

Figure 2 – Representative hysteretic response of embedded column base connection (Grilli et al. 2017)

3. Finite element model development and verification

In order to investigate the hysteretic response of steel columns embedded on column footings a FE model should be developed. This is done in two steps. In the first step, the FE model is validated with column specimens tested by Elkady and Lignos (2016, 2017a) that their base boundary was nominally fixed. Table 2 summarizes key features of the employed test specimens including the applied constant compressive axial load ratios (P is the applied axial load; $P_y = f_yA$; f_y is the expected yield stress; A is the column cross-section area) and the corresponding member slenderness, L_b/r_y (L_b and r_y are the unbraced length and the radius of gyration about weak-axis of the cross-section, respectively). Both fixed end and fix-flexible column specimens are considered. The FE model is developed in the commercial finite element analysis software ABAQUS (version 6.14-1) (ABAQUS 2014). Wide flange columns are modelled with shell elements based on the modeling approach discussed in Elkady and Lignos (2015, 2017a, 2017b). The material nonlinearity is considered with a combined isotropic/kinematic material hardening law (Lemaitre and Chaboche 1994) and residual stresses due to hot-rolling. Local and member geometric instabilities are triggered by assigning local and out-of-straightness geometric imperfections within the ASTM (2003) and AISC (2010b) limits.

Figures 3 illustrates comparisons of the column base moment, M_{base}, – chord rotation, θ, relations obtained from FE simulations and test results. The column base moment, M_{base}, is the reaction moment at the column bottom surface. The second order moment demand has been subtracted in all cases. The chord rotation, θ, is defined as the horizontal displacement at the top divided by

the actual column height, *L* by considering the corresponding column axial shortening if any. The comparisons suggest that the developed FE model simulates relatively well the test results throughout the entire loading history regardless of the employed cross-section and member end boundary conditions. Therefore, the FE model is deemed to be reliable and is further extended to assess the influence of the column base flexibility on the column hysteretic response.

Table 2 – Selected column specimens for the FE model development and verification (Elkady and Lignos 2016, 2017a)

Specimen ID	Cross-section	Slenderness ratio, L_b/r_y	Axial load ratio, P/P_y	Boundary conditions (Top-Bottom)	EI/L[*1] (10^5 kNm/rad)
C1	W24x146	79	20%	Fixed – Fixed	0.923
C2	W24x146	79	50%	Fixed - Fixed	0.923
C3	W24x146	79	20%	Flexible - Fixed	0.923
C7	W24x84	51	20%	Flexible - Fixed	0.488

[*1]*E*: Young's modulus of steel, and *I*: the second moment of inertia about strong axis
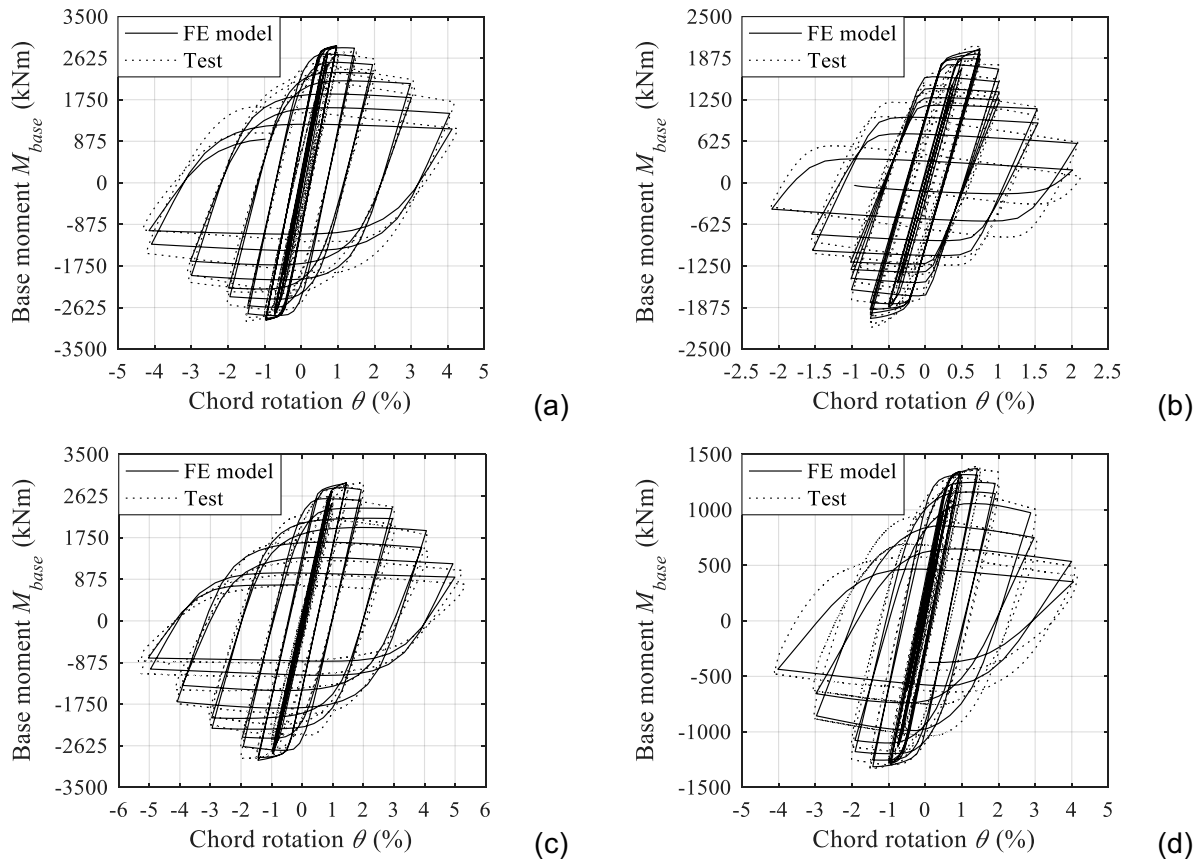

Figure 3 – Comparison between tests and FE simulations: (a) C1; (b) C2; (c) C3; and (d) C7. (data from Elkady and Lignos 2016, 2017a)

4. Refinement of finite element model boundary conditions

Figure 4 shows schematically the boundary conditions of a typical interior steel MRF column. In order to simulate the corresponding rotational stiffness attributed to the embedded column base connection, a rotational spring is assigned at the column base. The elastic stiffness, β of this spring is inferred based on the corresponding values of Table 1 (Grilli et al. 2017) by considering notional column sizes corresponding to the assumed column base connection strength.
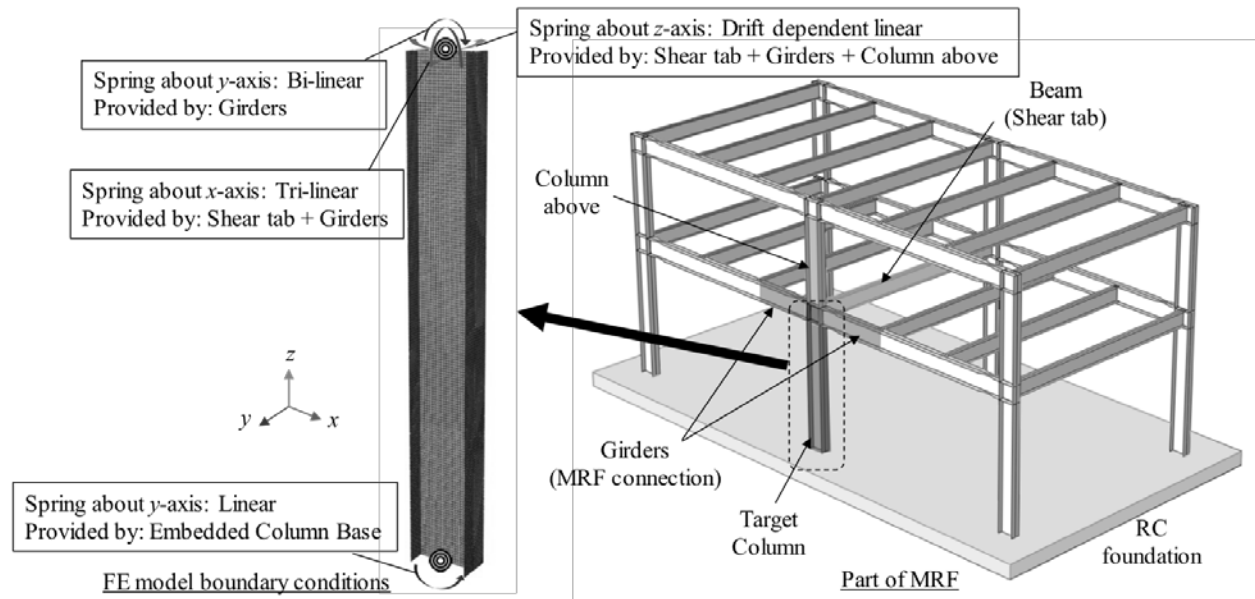

Figure 4 – Schematic representation of column end boundary conditions

Referring to Figure 4, three rotational springs are assigned at the column top to represent its member top end boundary conditions. The spring assigned with respect to the y-axis characterizes the in-plane rotational stiffness of the girders intersecting the column. A bilinear hysteretic response is assigned to this spring to consider the inelastic behavior of the steel girders. The rotational spring assigned with respect to the x-axis, represents the out-of-plane flexibility due to the shear tab beam-to-column connection (Liu and Astaneh-Asl 2000, 2004) and the torsional resistance of the girders. This spring is characterized by a tri-linear hysteretic behavior. A third spring is assigned at the column top end with respect to the z-axis that represents the torsional resistance due to bending of the shear tab plate, the torsional resistance of the 2nd story column and the weak-axis bending resistance of the girders. The contributions of these three components are lumped in a drift-dependent linear behavior that is idealized based on experimental findings summarized in Zhang and Ricles (2006). The authors plan to conduct further physical testing to characterize this relationship.

Prior experiments on beam-to-column connections that utilized deep columns and typical beams with reduced beam sections (RBS) (Chi and Uang 2002; Zhang and Ricles 2006) indicated that deep columns experience additional torque demands after the onset of severe local buckling within the RBS region. These demands are considered in the present study. In particular, the corresponding torque force – lateral drift relation is established on the basis of mechanics-based equations and experimental observations (Chi and Uang 2002; Zhang and Ricles 2006; Lignos et al. 2010; Lignos and Krawinkler 2012).

5. Parametric study to assess the effect of column base flexibility

A parametric study is conducted to evaluate the influence of the column base flexibility on the column performance based on the refined FE model discussed in Section 4. In all cases it is assumed that the concrete footing strength is sufficiently large such that the structural damage always occurs in the steel column. Table 3 and Figure 5 provides a summary of the investigated cases. Most of the employed cross-sections are highly ductile as per AISC-341-10 (AISC 2010a). Note that the rotational stiffness, β corresponding to the one deduced from experiments is referred as 'real' (Grilli et al. 2017). The AISC symmetric cyclic lateral loading protocol is employed in the context of this study.

Table 3 – Variables in the parametric study

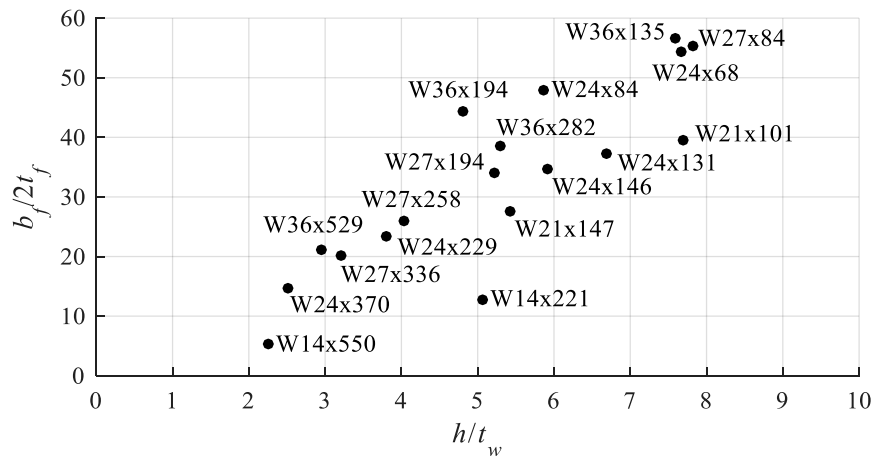| Column base rotational stiffness, β	Length L	Axial load ratio P/P_y	Cross-section
5 cases (Fixed, Real, 75%Real, 50%Real, Pin)	3 cases (3.0, 4.5, 6.0m)	4 cases (5, 20, 35, 50%)	18 cases (see Figure 5)

Figure 5 – Selected steel column cross-sections for the parametric study

6. Results and Discussion

6-1. Qualitative assessment of representative cases

Figure 6 shows the FE analysis results obtained from representative cases examined (i.e., W24x146-L4.5m-P/P_y=20%) with different column base flexibilities. Figure 6(a) shows a typical column base moment - chord rotation relation. The emphasis on this paper is on the maximum base moment, $M_{max}*$, corresponding to the capping rotation, $\theta_{max}*$, and the post-capping plastic rotation $\theta_{pc}*$ that characterizes the post-buckling behavior of a member. These parameters are commonly used in component deterioration models employed in nonlinear frame analysis (PEER/ATC 2010).

Figure 6(b) shows the influence of the assumed column base flexibility on the first-cycle envelope curve of a steel column. From this figure, while the column base flexibility increases, the onset of local buckling is delayed. Therefore, $\theta_{max}*$ increases while the column base stiffness decreases. Referring to Figure 6b, the rate of flexural strength deterioration, which is related to the local

buckling progression seems to be more or less the same regardless of the employed column base stiffness. This is to be expected because the concrete footing is assumed to remain elastic in the context of the present study. The maximum column base moment was found to be almost the same regardless of the column base flexibility. Note that the torque force demand applied at the column top did not practically influence the hysteretic response of the column for the considered lateral loading protocol. This is attributed to the fact that the column strength mostly deteriorated due to local buckling rather than lateral torsional buckling. FE simulations with asymmetric lateral loading histories indicate that lateral torsional buckling is strongly influenced by the torque force demand.
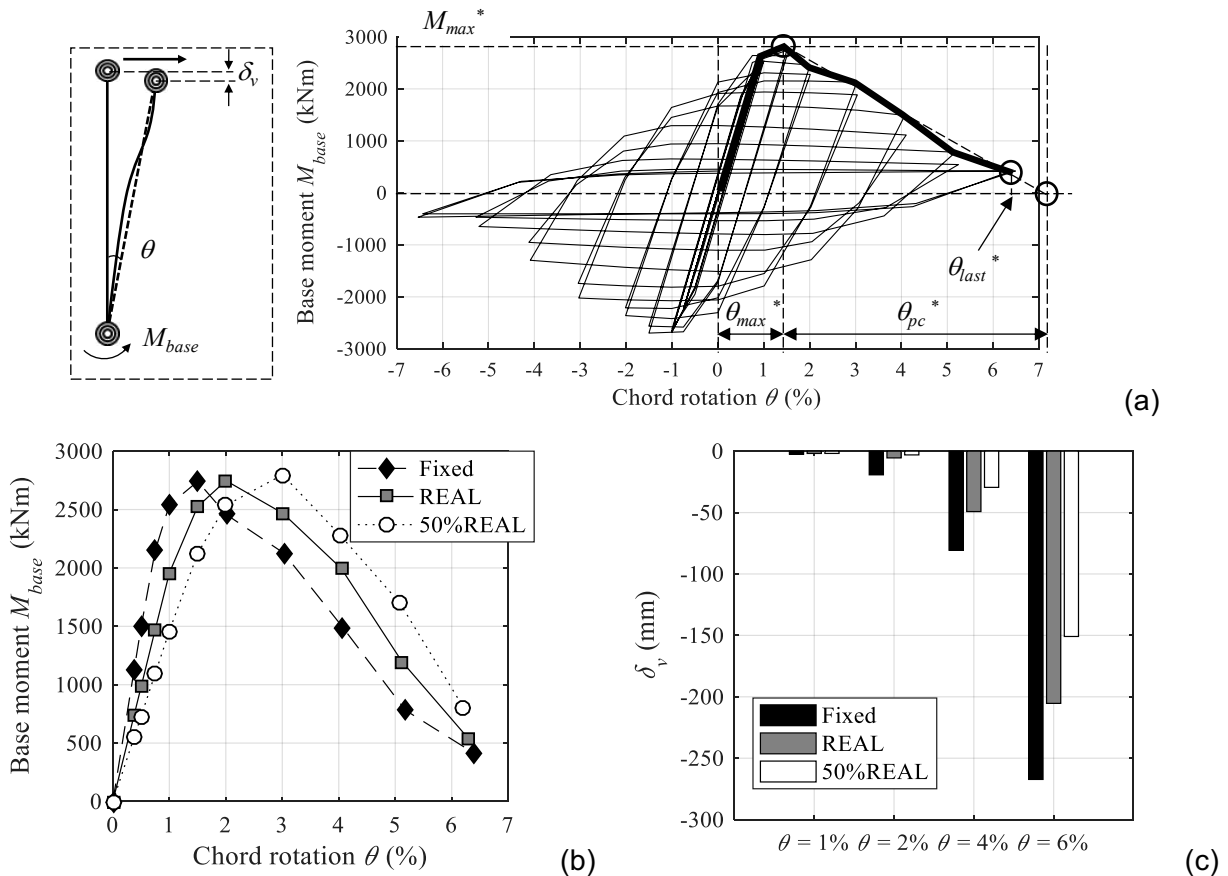

Figure 6 – FE analysis results of representative specimens (W24x146-L4.5m-P/P_y=20%): (a) Typical moment-rotation relation, (b) first-cycle envelope, and (c) vertical displacement of the column top

Figure 6(c) shows the influence of the column base flexibility on the vertical displacement of the column top, δ_v (see Figure 6(a)), which is strongly related to the observed axial shortening once local buckling occurs. δ_v is distinguished from axial shortening since the value of δ_v depends on the column dimensions. The figure suggests that the vertical displacement in a 'real' case is smaller than the nominally "fixed" column base case. For instance, at a reference chord rotation of 2% radians representative of design basis seismic events, the column axial shortening reduction is more than 50% compared to the "fixed" case. This is attributed to the fact that the cumulative plastic rotation in flexible column bases is smaller than that of a fixed base case at a given drift.

6-2. Capping rotation, $\theta_{max}*$

Figure 6(b) suggests that the capping rotation, $\theta_{max}*$ increases while the elastic concrete footing stiffness decreases. Prior research (Elkady and Lignos 2015) suggests that the pre-peak plastic rotation, θ_p* (i.e., $\theta_p* = \theta_{max}* - \theta_y$) increases exponentially while the local and/or global slenderness and/or the column axial load ratio decrease. Same observations hold true in the present study.

Figure 7 shows the $\theta_{max}*$ versus h/t_w relation for 4.5m long steel columns subjected to $P/P_y = 20\%$ with four different column base flexibilities. The FE simulations suggest that if the concrete footing stiffness decreases then $\theta_{max}*$ increases in most cases. This finding hold true regardless of the member length and the applied axial load ratio. For all practical purposes, the $\theta_{max}*$ increase compared to the ideally "fixed" condition may be approximated as 0.5% radians for the 'real' case and 1.0%rad for the '50% of real' case.
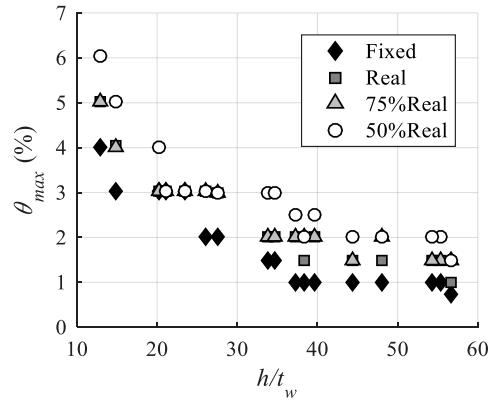

Figure 7 – Capping plastic rotation, $\theta_{max}*$ – web local slenderness ratio relation (L4.5m-P/P_y=20%)

6-3. Post-capping plastic rotation, $\theta_{pc}*$

Figure 6(b) indicates that the post-capping plastic rotation, $\theta_{pc}*$ is practically not influenced by the column base flexibility given that the column base strength is assumed to be infinite (i.e., elastic concrete footing). Therefore, regardless of the employed column base flexibility, the predictive equations proposed by Hartloper and Lignos (2017) may be adopted. Note that the deduced $\theta_{pc}*$ values are in the range of 5-10% radians if P/P_y =20% and 20 < h/t_w < 45. At higher axial load ratios and/or higher h/t_w ratios, the $\theta_{pc}*$ values range between 2-5%radians.

6-4. Column axial shortening, δ_{axial}

In order to assess the column axial shortening among models with different length, the vertical displacement at the column top of each model, δ_v, is subtracted by the vertical displacement of same model with pinned column base, $\delta_{v,pin}$. Therefore axial shortening, $\delta_{axial}* = \delta_v - \delta_{v,pin}$.

Figure 8 shows the $\delta_{axial}*$ - h/t_w relation for different column lengths and column base flexibilities. In general, the observed axial shortening at a given rotation is slightly smaller for longer columns because the yield rotation is larger due to the smaller column flexural stiffness. However, column axial shortening is almost the same regardless of the column length. The reason is that column

axial shortening mainly depends on the onset of local buckling, which in turn depends on the employed cross-sectional properties.

Referring to Figure 8(b) the column axial shortening is shown at characteristic drift demands. Notably, at a drift of 2% the column axial shortening is minor if the column base flexibility is considered. In that respect, the column-base 'fixed' assumption is fairly conservative. From the same figure, if a 50% reduction of the real column base flexibility is assumed, the corresponding axial shortening at a lateral drift of 2% is almost zero in most of the cases. Similarly, if a 50% reduction of the real column base flexibility is assumed, the corresponding axial shortening reduction is, 80% and 30% at a lateral drift of 2% and 4%, respectively.
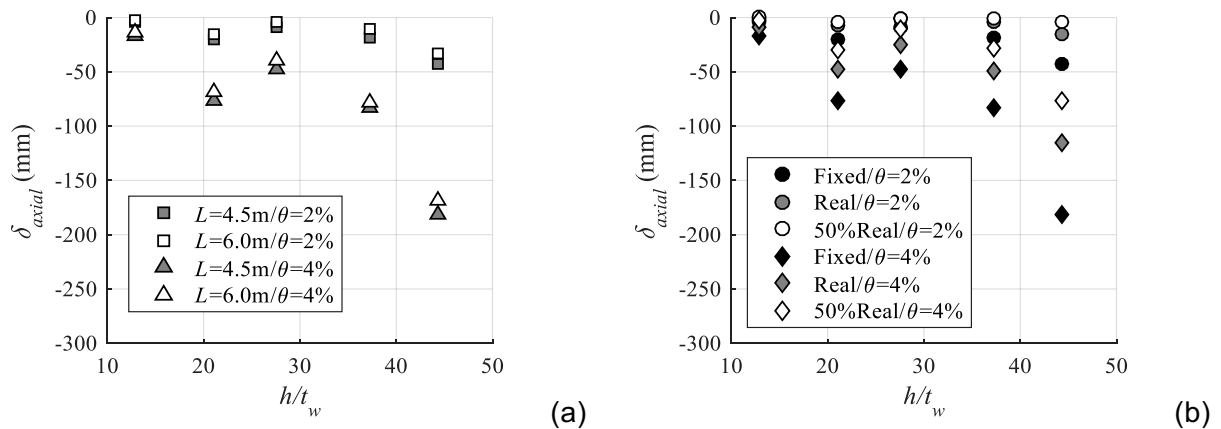

Figure 8 – Column axial shortening – web local slenderness ratio relation:(a) P/P_y=20% and β = Fixed and (b) P/P_y=20% and L = 4.5m

7. Summary and Conclusions

This paper investigated the influence of the column base flexibility on the hysteretic behavior of first story interior wide flange steel columns typically seen in moment-resisting frames (MRFs). This was achieved through a parametric study that was conducted with rigorous finite element (FE) simulations. The parameters that were investigated include the column base flexibility, the applied axial load ratio and the geometric properties of the employed cross-section. The developed FE model was validated with representative test results from full-scale steel column experiments. The boundary conditions of the FE model were further refined to reflect representative column base connection flexibilities inferred from recent full-scale embedded column base tests. The main findings are summarized as follows,

1. The corresponding capping rotation, $\theta_{max}*$ increases while the elastic stiffness of the column base foundation decreases. This increase is on average, 0.5% radians when the 'real' column base flexibility is considered relative to the nominally fixed-base case. The corresponding, $\theta_{max}*$ increases by 1.0%rad if the 'real' column base flexibility is reduced by 50%. It was also found that the influence of the column base flexibility on the post-capping rotation, $\theta_{pc}*$ was practically negligible.
2. The column axial shortening is overestimated if the embedded column base flexibility is neglected. In particular, the FE simulation results suggest that the column axial shortening reduction relative to the theoretically 'fixed' base can be more than 30% at a reference lateral drift demand of 4%.

Acknowledgments

References

ABAQUS. (2014). *ABAQUS analysis user's manual version 6.14-1.* Dassault Systems Simulia Corp., RI, USA.

AISC. (2010a). *Seismic Provisions for Structural Steel Buildings. ANSI/AISC-341-10.* American Institute of Steel Construction.

AISC. (2010b). *Specification for Structural Steel Buildings. ANSI/AISC 360-10.* American Institute of Steel Construction.

ASTM. (2003). Standard Specification for General Requirements for Rolled Structural Steel Bars, Plates, Shapes, and Sheet Piling. American Society for Testing and Materials.

Chi, B., and Uang, C. M. (2002). Cyclic Response and Design Recommendations of Reduced Beam Section Moment Connections with Deep Columns. *Journal of Structural Engineering*, *128*(4), 464–473.

Clifton, G. C., Bruneau, M., MacRae, G. A., Leon, R., and Fussell, A. (2011). Steel Structures Damage from the Christchurch Earthquake Series of 2010 and 2011. *Bulletin of the New Zealand Society for Earthqauke Engineering*, *44*(4), 297–318.

Elkady, A., and Lignos, D. G. (2015). Analytical investigation of the cyclic behavior and plastic hinge formation in deep wide-flange steel beam-columns. *Bulletin of Earthquake Engineering*, *13*(4), 1097–1118.

Elkady, A., and Lignos, D. G. (2016). Dynamic Stability of Deep and Slender Wide-Flange Steel Columns - Full Scale Experiments. *Proceedings of the Annual Stability Conference Structural Stability Research Council*.

Elkady, A., and Lignos, D. G. (2017a). Full-Scale Cyclic Testing of Deep Slender Wide-Flange Steel Beam-Columns under Unidirectional and Bidirectional Lateral Drift Demands. *16th World Conference on Earthquake Engineering (16WCEE), Santiago, Chile*, num. 944.

Elkady, A., and Lignos, D. G. (2017b). Stability Requirements of Deep Steel Wide-Flange Columns under Cyclic Loading. *Proceedings of the Annual Stability Conference Structural Stability Research Council, San Antonio, Texas*.

Fogarty, J., and El-Tawil, S. (2016). Collapse Resistance of Steel Columns under Combined Axial and Lateral Loading. *Journal of Structural Engineering*, *142*(1), 4015091.

Grilli, D. A., Jones, R., and Kanvinde, A. M. (2017). Seismic Performance of Embedded Column Base Connections Subjected to Axial and Lateral Loads. *Journal of Structural Engineering*.

Hartloper, A., and Lignos, D. G. (2017). Updates to the ASCE-41-13 Provisions for the Nonlinear Modeling of Steel Wide-Flange Columns for Performance-Based Earthquake Engineering. *EUROSTEEL 2017, Copenhagen, Denmark*.

Ibarra, L. F., and Krawinkler, H. (2005). *Global Collapse of Frame Structures under Seismic Excitations. John A. Blume Earthquake Engineering Center Technical Report 152. Stanford Digital Repository.* Available at http://purl.stanford.edu/dj885ym2486

Lemaitre, J., and Chaboche, J.-L. (1994). *Mechanics of solid materials*. Cambridge university press.

Lignos, D. G., Hikino, T., Matsuoka, Y., and Nakashima, M. (2013). Collapse Assessment of Steel Moment Frames Based on E-Defense Full-Scale Shake Table Collapse Tests. *Journal of Structural Engineering*, *139*(1), 120–132.

Lignos, D. G., Kolios, D., and Miranda, E. (2010). Fragility assessment of reduced beam section moment connections. *Journal of Structural Engineering, 136*(9), 1140–1150.

Lignos, D. G., and Krawinkler, H. (2012). Development and utilization of structural component databases for performance-based earthquake engineering. *Journal of Structural Engineering*, *139*(8), 1382–1394.

Liu, J., and Astaneh-Asl, A. (2000). Cyclic Testing of Simple Connections Including Effects of Slab. *Journal of Structural Engineering*, *126*(1), 32–39.

Liu, J., and Astaneh-Asl, A. (2004). Moment–Rotation Parameters for Composite Shear Tab Connections. *Journal of Structural Engineering*, *130*(9), 1371–1380.

MacRae, G. A., Clifton, G. C., Bruneau, M., Kanvinde, A. M., and Gardiner, S. (2015). Lessons from Steel Structures in Christchurch Earthquakes. *Proceedings of the 8th International Conference on Behavior of Steel Structures in Seismic Areas (STESSA), Shanghai, China*.

Newell, J. D., and Uang, C.-M. (2008). Cyclic Behavior of Steel Wide-Flange Columns Subjected to Large Drift. *Journal of Structural Engineering*, *134*(8), 1334–1342.

PEER/ATC. (2010). Modeling and acceptance criteria for seismic design and analysis of tall buildings, PEER/ATC 72–1. Prepared for Pacific Earthquake Engineering Research Center (PEER) by Applied Technology Council (ATC), Redwood City, San Diego.

Suzuki, Y., and Lignos, D. G. (2015). Large Scale Collapse Experiments of Wide Flange Steel Beam-Columns. *Proceedings of the 8th International Conference on Behavior of Steel Structures in Seismic Areas (STESSA), Shanghai, China.*

Uang, C. M., Ozkula, G., and Harris, J. (2015). Observations from cyclic tests on deep, slender wide-flange structural. *Proceedings of the Annual Stability Conference Structural Stability Research Council, Tennessee, Nashville.*, 247–263.

Zareian, F., and Kanvinde, A. (2013). Effect of Column-Base Flexibility on the Seismic Response and Safety of Steel Moment-Resisting Frames. *Earthquake Spectra*, *29*(4), 1537–1559.

Zhang, X., and Ricles, J. M. (2006). Experimental Evaluation of Reduced Beam Section Connections to Deep Columns. *Journal of Structural Engineering*, *132*(3), 346–357.